EXPERIMENTAL DETECTION OF DEBONDING OF PIEZOTRANSDUCERS WITH THE SEGMENTED ELECTRODE

ABSTRACT

The piezoelectric transducers (PZT) are bonded to smart structures by means of an intermediate adhesive layer, with the main objectives of applying methodologies of structural health monitoring, nondestructive evaluation, nondestructive inspection and structural control to the structures. However, the application of these methodologies depends on the health of the adhesive joint that couples mechanically the PZT with the structure. This research shows an experimental technique based on the segmentation of electrodes of a PZT patch in sheet form. One electrode is segmented in three equal parts (end left, middle and end right) to obtain three electrical signatures of a PZT. The electrical signatures (voltage) of the end electrodes are related to the middle electrode voltage. Three experiments were carried out in this study: two static cases and one dynamic case. For the static case, the left end (first case) and the right end (first case) were debonded. In the dynamic case, only one side was debonded. The results show that the voltage relations present linear behavior and the changing in the slope of the voltage ratio allows identifying which electrode is debonded. This technique showed to be effective in the three studied cases of debonding and it could be used to identify debonding in real time.

KEYWORDS: Debonding detection, piezoelectric transducers, segmented electrode, structural health monitoring.

HECTOR A. TINOCO
Mechanical Engineer, M.Sc.
Universidad Autónoma de Manizales-UAM, Colombia
htinoco@autonoma.edu.co

ALBERTO L. SERPA
Mechanical Engineer, Ph.D.
Professor
University of Campinas
UNICAMP-Brazil
serpa@fem.unicamp.br

1. INTRODUCTION

Piezoelectric transducers of Lead Zirconate Titanate (PZT) are used in structural engineering to apply monitoring methodologies in different types of structures, such as civil structures [1], aerospace structures [2], and among others [3]. Some methodologies applied are structural health monitoring (SHM) and nondestructive evaluation (NDE) and these depend on the health of piezoelectric transducers to apply the monitoring tasks.

Usually, the piezoelectric transducers used for SHM and NDE are bonded with an adhesive layer to the host structure that will be either monitored or evaluated. Adhesive layer applied provides the mechanical coupling in order to transfer the mechanical forces through it. Adhesive layer is considered an interfacial layer of finite thickness which is applied between the piezoelectric element and host structure (see Fig. 1).

Some techniques that use PZT in structures for detection, identification, quantification and damage localization are: EMI technique [4, 5-6], Lamb-wave-based techniques in SHM methodologies [7] and others. The application and reliability of the different techniques depend on the health of sensors and actuators, due to that the electrical signatures emitted by transducers can be influenced either by the properties of mechanical coupling (geometric and physical properties of the adhesive layer) or by the debonding of the piezoelectric transducers. Despite that the geometrical properties of the adhesive layer influence the electrical signatures and it produces mechanical effects in the set (host structure, adhesive and PZT) these have been studied to show that its effects can be controlled in the design (see [8]). Therefore, major attention has been paid in the last few years on the debonding of piezoelectric transducers.

A study carried out by [9] shows that the control of smart structures can be affected by the occurrence of debonding. An analytical and experimental investigation was carried out to identify the effects of delamination on smart beams with bonded piezoelectric actuators [10], and the results of this study showed that edge delaminations origin a decreasing in the natural frequency, however the interior delaminations do not produced change. The study carried out by [11] also showed that debonding effects influence the electrical impedance of the piezoelectric sensors. These authors established an algorithm for detecting debonding using optimization and these results can be applied in the EMI technique. In addition, [12] showed, by means of simulation that when active control is applied to smart beams, the effects of debonding of an actuator can significantly affect the passive and hybrid control. Recently, [13] provided a comprehensive theoretical study of the effects of the debonding on the dynamic behavior of piezoelectric actuators. Results showed that debonding defects modify the electromechanical coupling between the host structure and the piezoelectric actuator. In advance, a numerical study was carried out to show that the electrical performance of partially

Fecha de Recepción: (Letra Times New Roman de 8 puntos)
Fecha de Aceptación: Dejar en blanco

debonded sensors is diminished cause by the debonding [8].

Further, [14] showed how the electrical performance of a piezoelectric sensor can be related to the debonding by means of the electrical power consumption of an electric circuit coupled to the set host structure, adhesive and piezoelectric sensor. This study analyzes how the power consumption can indicate debonding and how a piezoelectric sensor can be monitored by its electrical performance. Another method of debonding detection was proposed by [15], where a modified electro-mechanical impedance model of PZT actuator-sensor was proposed. The results of a modified model showed that if the bonding quality is reduced, the natural frequencies are modified and the frequency response augments its amplitude, as well as the EMI spectrum was perturbed with noise. A numerical example demonstrated the feasibility to use the modified model for debonding detection of piezoelectric patches.

Recently, [16] shows a new method to monitor debonding of piezoelectric sensors, which consists of segmenting the electrode of a piezoelectric sheet in three parts. Voltage relations between the segmented electrodes show a linear behavior and these relations correspond to force relations in electrodes, respectively. The results showed that if debonding happens, the force relations in electrodes are influenced and the voltage relations vary. The technique was explained analytically. This research shows an experimental study that verifies if the voltage relations are linear in electrodes. Further, voltage relations can help to identify edge delaminations as it was proposed by [16]. This study shows that the changing in the slope of linear relations indicates that one end of the electrode presents debonding. The proposed technique by [16] could be used for monitoring the bonding of piezoelectric sheets bonded to structures in an operational state.

2. THEORETICAL PRINCIPLES [16]

2.1 Equilibrium Equations

The set shown in Fig. 1 is composed of a piezoelectric sensor bonded to a host structure by means of an adhesive layer, which is submitted to external forces.

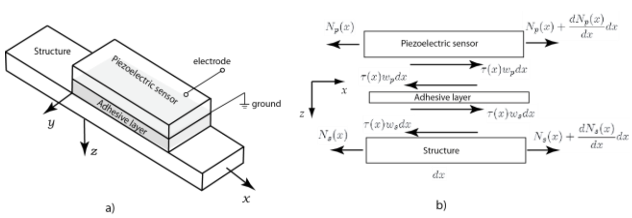

Figure 1. (a) Set structure, adhesive layer and piezoelectric-sensor. (b) Infinitesimal element dx of the set structure, adhesive layer and piezoelectric sensor [16].

The lengths of the piezoelectric sensor l_p and the structure l_s are finite along $x-$axis and these are assumed to be equal. The width of the set is denoted by w (along $y-$axis) and the thickness by h (along $z-$axis). Subscripts s, p and a indicate structure, piezoelectric sensor and adhesive layer, respectively. The notation of subscripts is applied to all geometric and physical parameters defined. From Fig. 1 the equilibrium equations for the set are obtained, such that

$$\begin{aligned}\frac{d^2u_s(x)}{dx^2} - \frac{G_a}{h_a E_s h_s} u_s(x) &= -\frac{G_a}{h_a E_s h_s} u_p(x), \\ \frac{d^2u_p(x)}{dx^2} - \frac{G_a}{h_a E_p h_p} u_p(x) &= -\frac{G_a}{h_a E_p h_p} u_s(x),\end{aligned} \tag{1}$$

where $u_p(x)$ and $u_s(x)$ are the displacements, E_p and E_s are the elasticity modulus of the sensor and the structure. Equilibrium equations of Eq. (1) were solved by [16].

2.1 Voltage Relations

The electro-mechanical coupling of piezoelectric materials is expressed by constitutive laws (see [17]) of the following form

$$\begin{aligned}\varepsilon_p &= s^E_{pq}\sigma_q + d_{kp}\Phi_k, \\ D_i &= d_{ik}\sigma_k + e^{\sigma}_{ik}\Phi_k,\end{aligned} \tag{2}$$

Where $D_i\left[C/m^2\right]$ is electric displacement, ε_p is the strain vector (dimensionless), $\Phi_k\left[V/m\right]$ is the applied electric field vector, $\sigma_k\left[N/m^2\right]$ is the mechanical stress vector, $e^{\sigma}_{ik}\left[F/m\right]$ is the electric permittivity to constant stress, $d_{kp}\left[C/N\right]$ and $d_{ik}\left[C/N\right]$ are piezoelectric strain coefficients, and $s^E_{pq}\left[m^2/N\right]$ is the elastic compliant to constant electric field.

The piezoelectric sensor showed in Fig. 2 has the segmented electrode in the top part. The electrode is divided in three equal parts. In order to obtain voltages in each electrode (e_{1L}, e_1 and e_{1R}), according to [18], the electric potential is determined for each electrode (V_1, V_2 and V_3) considering that each electrode acts as a capacitor, so we have that

$$\begin{aligned}V_1 &= \kappa\int_0^{l_1}(\varepsilon^x_s(x) - \varepsilon^x_p(x))dx, \\ V_2 &= \kappa\int_{l_1}^{l_2}(\varepsilon^x_s(x) - \varepsilon^x_p(x))dx, \\ V_3 &= \kappa\int_{l_2}^{l_3}(\varepsilon^x_s(x) - \varepsilon^x_p(x))dx,\end{aligned} \tag{3}$$

where $\kappa = \dfrac{d_{15} G_a w_p h_p}{h_a C_p}$, $\varepsilon_s^x(x)$ and $\varepsilon_p^x(x)$ are strains.

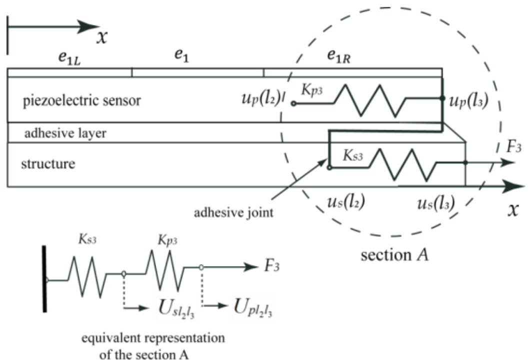

Figure 2. Equivalent system of springs for the set structure, adhesive layer and piezoelectric sensor [16].

Figure 2 shows a set in which the piezoelectric patch has divided its electrode in three equal parts. In each segmented electrode we consider that there is two springs coupled in series of stiffness K_s (structure) and K_p (piezoelectric). The spring system presents linear behavior and it is established to approximate the displacements of each electrode and of each section of the structure. Therefore, it is assumed that each section e_{1L}, e_1 and e_{1R} can be represented by

$$F_1 = K_{p1} U_{pl_1} = K_{s1} U_{sl_1},\ F_2 = K_{p2} U_{pl_1 l_2} = K_{s2} U_{sl_1 l_2},\ F_3 = K_{p3} U_{pl_2 l_3} = K_{s3} U_{sl_2 l_3}. \quad (4)$$

It is important to point out that if the lengths of the electrodes are the same, we can assume that $K_{s1} = K_{s2} = K_{s3} = K_s$ and $K_{p1} = K_{p2} = K_{p3} = K_p$. Then, Eq. (4) is introduced in Eq. (3) and the following relations are obtained

$$V_1 = \frac{\left(\frac{1}{K_s} - \frac{1}{K_p}\right) F_1}{\left(\frac{1}{K_s} - \frac{1}{K_p}\right) F_2} V_2,\ V_3 = \frac{\left(\frac{1}{K_s} - \frac{1}{K_p}\right) F_3}{\left(\frac{1}{K_s} - \frac{1}{K_p}\right) F_2} V_2. \quad (5)$$

Reorganizing Eq. (5), we determine that

$$V_1 = \mu_1 V_2,\ V_3 = \mu_3 V_2, \quad (6)$$

where $\mu_1 = F_1 / F_2$ and $\mu_3 = F_3 / F_2$ are the force relations in electrodes. Those relations are directly proportional to the voltage of the middle electrode. Equation (6) shows that the electric potentials of the electrodes of the extremity are linear functions. Their slopes are the force relations in electrodes.

3. EXPERIMENTAL TEST

In these experimental tests are evaluated the voltage relations in three cases, two static cases and one dynamic case. For both cases (static and dynamic) the applied forces are random, due to that the theory exposed by [16] demonstrates that the voltage relations do not depend on external forces. The following materials are used for the experimental tests:

1. Adhesive: Epoxi resin.
2. Structure: Aluminium.
3. Data acquisition card (dSPACE).
4. Piezoelectric transducer (PZT-5H).
5. Software: MATLAB.

For the static test the forces applied are provided by a device called press. The segmentation of electrodes was carried on the top electrode that covers one side of the piezoelectric patch. Simply, the segmentation is a created discontinuity in the electrode. The top electrode was segmented in three equal parts, for the three specimens. Other works have used the segmentation of electrodes for energy harvesting, which are [19-20].

3.1 Static Test for Specimens 1 and 2

Figure 3 shows the configuration for the specimens used in the static test. The specimen number 1 presents debonding in the left edge (see Table 1) and the specimen number 2 presents it in the right edge (see Table 2).

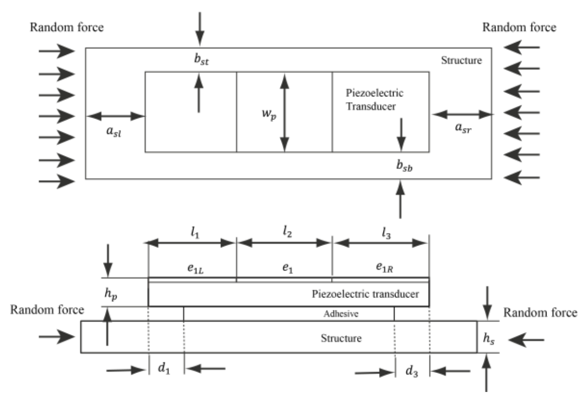

Figure 3. Characteristics of the specimens.

The applied forces to the specimens are random, since [16] explain that the voltage relations do not depend on external forces. Then, the principal aim is to identify that the side is debonded in the specimens using the voltage relations between electrodes.

specimen	d_1	d_3	h_s	a_{sr}	a_{sl}	b_{st}	b_{sb}	w_p	h_p	l_1	l_2	l_3
1	5	0	2	32	32	1	2.5	11	0.3	10	10	10

Table 1. Dimensions in *mm* of the specimen 1: static case (see Fig.3).

specimen	d_1	d_3	h_s	a_{sr}	a_{sl}	b_{st}	b_{sb}	w_p	h_p	l_1	l_2	l_3
2	0	3	3	20	20	0	0	10	0.3	6.5	6	6.5

Table 2. Dimensions in *mm* of the specimen 2: static case (see Fig.3).

Figure 4 shows the results obtained for the voltage relations in electrodes when applied random external forces in the specimen number 1. The results for the slopes V1 and V3 indicate that the force relations for e_{1L} and e_{1R} are $\mu_1 = 2.46$ and $\mu_2 = 3.36$ times the force of the middle electrode (see Eq. (6)). The slope indicates the force relation in electrodes as described by [16]. This test confirms that the voltage relation in electrodes have a linear behavior (see Eq. (6)). Further, it is possible to identify which electrode is debonded, as explained by [16], where the voltage relation (slope) that is smaller will indicate debonded. This is due to the fact that initially the voltage relations are equal and when the electrode is debonded the adhesive coupling loses stiffness (see Eq. (4)). Therefore, in this case we can identify that the left electrode is debonded ($\mu_1 < \mu_2$). For this test the induced debonding is 5 *mm*. The slopes were obtained using linear approximations with correlation coefficients of 0.992 and 0.996 for V1 and V3.

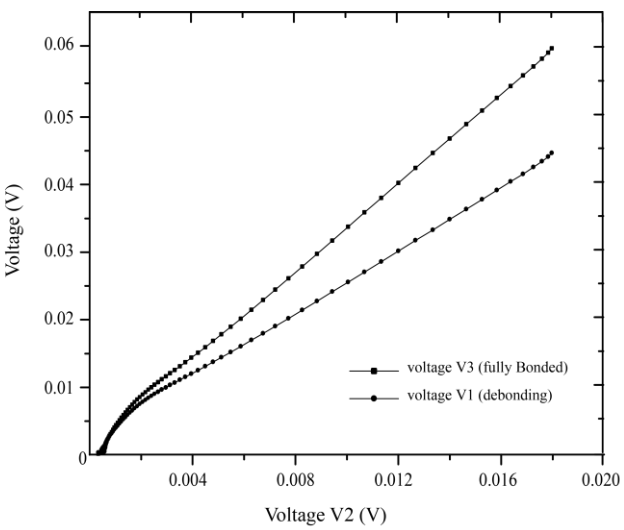

Figure 4. Characteristics of the specimens.

The same procedures that for the specimen number 1 were carried out for the specimen number 2. The results obtained from the voltage relations in electrodes are shown in Fig. 5. The slopes V1 and V3 indicate that the force relations for e_{1L} and e_{1R} are $\mu_1 = 0.598$ and $\mu_2 = 0.432$ times the force of the middle electrode. Similar to the test number 1, the voltage relations are linear. Hence, we can identify that the electrode e_{1R} is debonded, since it presents a smaller slope than the electrode e_{1L} . Then, it is possible conclude that $\mu_2 < \mu_1$. The correlation coefficients for the linear approximations are 0.999 and 0.999 for V1 and V3. The length of debonding induced was of 3 *mm.*

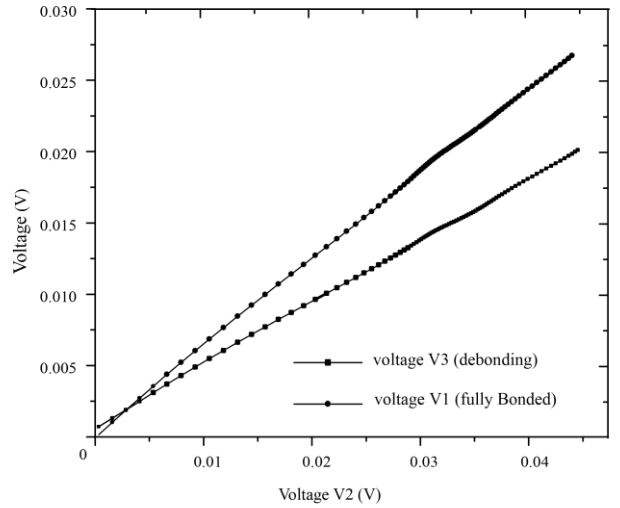

Figure 5. Characteristics of the specimens.

In both cases the prediction provided by voltage ratio was correct. In each case, the electrode that presented smaller voltage ratio was debonded. In piezoelectric patches the probability that the debonding occurs in the ends is due to that the shear stresses are bigger there than along the patches, as explained by [8].

3.2 Dynamic Test: Especimen 3

In this experimental test was used a data acquisition card USB 6211 National Instruments, the information was obtained by means of an algorithm made in MATLAB.

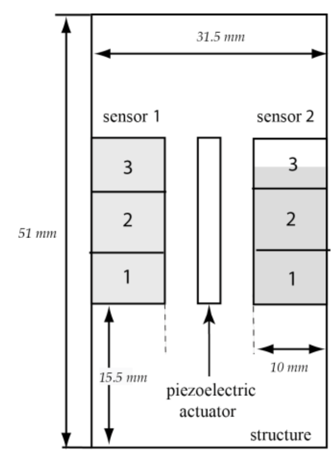

Figure 6. Characteristics of the specimen.

Two piezoelectric patches with the segmented electrode were bonded to host structure as shown in Fig. 6. However, one patch presents debonding in the electrode number 3 and another patch is fully bonded. Between both patches, an actuator is located for exciting the structure and so, to get measures of voltage in each sensor. The voltage function applied to the actuator was chosen as

$$V(t) = 8\sin(\omega t)\,[\mathrm{V}]. \quad (7)$$

For Eq. (7) ω is the frequency and t the time. Table 3 shows the geometric properties of the specimen used in this test.

PZT	d_1	d_3	h_s	w_p	h_p	l_1	l_2	l_3	h_a
1	0	0	2	11	0.3	10	10	10	0.3
2	0	2	0.3	10	0.3	4	4	4	0.2

Table 3. Dimensions in *mm* of the specimen 3: dynamic case (see Fig.6).

For the sensor 1 (sensor fully bonded) the values of force relations obtained are $\mu_1 = 0.97$, $\mu_2 = 0.98$ and these were approximated from voltages obtained of the sensor 1 (voltages in each electrode). Those values were calculated using a linear regression. The voltage ratio functions are shown in Fig. 7. The values μ_1 and μ_2 determine that the slopes are parallel; this means that voltage relations are approximately equal.

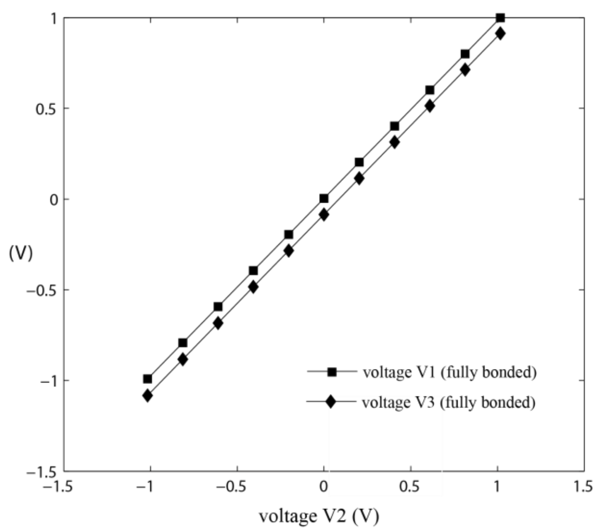

Figure 7. Voltage ratios obtained from the sensor 1, sensor fully bonded.

Figure 7 demonstrates that if voltage ratios are equal, the mechanical coupling means fully bonded. In the contrary case, we can identify some changes in the mechanical coupling when the debonding take place.

For the sensor 2 (sensor partially bonded) the values of force relations obtained are $\mu_1 = 1.15$, $\mu_2 = 0.1426$ and those were approximated from voltages obtained of the sensor 2 (voltages in each electrode). A linear regression was applied for determining the voltage ratio functions shown in Fig. 8. The values μ_1 and μ_2 determine that electrode is debonded, such that $\mu_2 < \mu_1$. Therefore, we can conclude that the electrode 3 of the sensor 2 presents partial debonded, but it is not possible to quantify the value on it. In this case is evidenced that the methodology proposed by [16] works in the dynamic case, and this methodology helps to identify existence of debonding in the edges of piezoelectric patches.

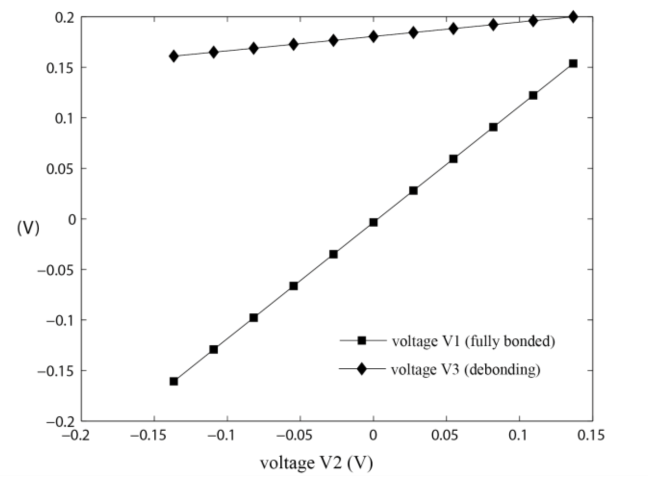

Figure 8. Voltage ratios obtained from the sensor 2, sensor partially bonded.

4. CONCLUSIONS

In this research the segmentation of electrodes of piezoelectric patches was proposed to detect the debonding of it. However, the detection is limited only to the debonding of edges. Further, this study showed that voltage ratio in electrodes presents a linear behavior.

In three proposed cases for the experimental tests performed, the technique of segmentation of electrodes in three parts show to be effective to identify which electrode was debonded. Therefore, it is possible that this technique can be used in operational state, since the results were similar for the dynamic and static cases. Also, some effects should be studied and understood, such as effects on the lateral debonding and which are the effects of the ratio in the length and the width of the patches to apply the proposed technique.

6. REFERENCES

[1] R. Tawie, and Lee H. K., "Monitoring the strength development in concrete by EMI sensing technique," *Construction and Building Materials*, Vol. 24, pp. 1746–1753, 2010.

[2] W. J. Taszewski, S. Mahzan, and R. Traynor, "Health monitoring of aerospace composite structures–active and passive approach," *Composites Science and Technology*, Vol. No. 69, No.11, pp. 1678-1685, 2009.

[3] W. Yan, and W.Q. Chen, "Structural health monitoring using high-frequency

electromechanical impedance signatures," *Advances in Civil Engineering*, pp. 1-11, 2010

[4] W. Yan, C. W. Lim, J. B. Cai, and W. Q. Chen, "An electromechanical impedance approach for quantitative damage detection in Timoshenko beams with piezoelectric patches," *Smart Materials and Structures*, Vol. 16, No. 4, pp. 1390–1400, 2007.

[5] C. T. Ng, and M. Veidt, "A Lamb-Wave based technique for damage detection in composite laminates," *Smart Materials and Structures*, Vol. 18 No. 7, pp. 1-12, 2009.

[6] V. G. M. Annamdas; and C. K. Soh, "Three dimensional electromechanical impedance model II: damage analysis and PZT characterization," *Journal of Aerospace Engineering*, Vol. 20, No. 1, pp. 63–71, 2007.

[7] S. Bhalla, and C.K. Soh, "Structural health monitoring by piezo-impedance transducers: Modeling," *Journal of Aerospace Engineering ASCE*, Vol. 17, No. 4, pp. 154–165, 2004.

[8] H. A. Tinoco, A. L. Serpa, and A: M. Ramos, "Numerical study of the effects of bonding layer properties on electrical signatures of piezoelectric sensors," *Mecánica Computacional*, Vol. 29, No. 86, pp. 8391-8409, 2010.

[9] C. E. Seeley, and A. Chattopadhyay, "Modeling delaminations in smart composite laminates," In: *Proceedings of the 37th structures, structural dynamics and materials conference*, Salt Lake City, United States, pp. 109–19. 1996.

[10] S. J. Kim, and J.D Jones, "Effects of piezo-actuator delamination on the performance of active noise and vibration control system," *Journal of Intelligent Material System and Structures*, Vo. 7, pp. 668–676, 1996.

[11] N. Saint-Pierre, Y. Jayet, I. Perrissin-Fabert, and J. C. Baboux, "The influence of bonding defects on the electric impedance of piezoelectric embedded elements," *Journal of Physics D (Applied Physics)*, Vol. 29, pp. 2976-2982. 1996.

[12] D. Sun, and L. Tong, "Effect of debonding in active constrained layer damping patches on hybrid control of smart beams," *International Journal of Solids and Structures*, Vol. 40, pp. 1633-1651, 2003.

[13] C. Jin, X. D. Wang, and M. J. Zuo, "The dynamic behaviour of surface-bonded piezoelectric actuators with debonded adhesive layers," *ActaMechanica*, Vol. 211, No. 3-4, pp. 215-235. 2010

[14] H. A. Tinoco, A. L. Serpa, and F. M. Peña, "Debonding estimation of piezoelectric sensors by power consumption analysis in smart structures using the finite element method," In: *Proceedings of V Congreso Internacional de Ingeniería Mecánica y III de Ingeniería Mecatronica*, Bogotá, Colombia, pp. 1-12, 2011.

[15] Y. G. Xu, and G. R. Liu, "A modified electro-mechanical impedance model of piezoelectric actuator-sensors for debonding detection of composite patches," *Journal of Intelligent Material Systems and Structures*, Vol. 13 No. 6, pp. 389–396, 2002.

[16] H. A. Tinoco, and A. L. Serpa, "Voltage relations for debonding detection of piezoelectric sensors with segmented electrode," *Mechanical System and Signal Processing*, Vol. 31, pp. 258-267, 2012.

[17] C. K. Lee, "Theory of laminated piezoelectric plates for the design of distributed sensors/actuators part I: Governing Equations and Reciprocal Relationships," *Journal of the Acoustical Society of America*, Vol. 87, No. 3, pp. 1144-1158. 1990.

[18] J. Sirohi, and I. Chopra, "Fundamental understanding of piezoelectric strain sensors," *Journal of Intelligent Material Systems and Structures*, Vol. 11, No. 4, pp. 246-257, 2000.

[19] Jr. C. De Marqui, A. Erturk, and D. J. Inman, "Piezoaeroelastic modeling and analysis of a generator wing with continuous and segmented electrodes," *Journal of Intelligent Material Systems and Structures*, Vol. 21, No. 10, pp. 983-993, 2010.

[20] A. Erturk, P. Tarazaga, J. R. Farmer, and Inman, "Effect of strain nodes and electrode configuration on piezoelectric energy harvesting from cantilevered beams," *Journal of Vibration and Acoustics*, Vol. 131, No. 1, pp. 1-11, 2009.